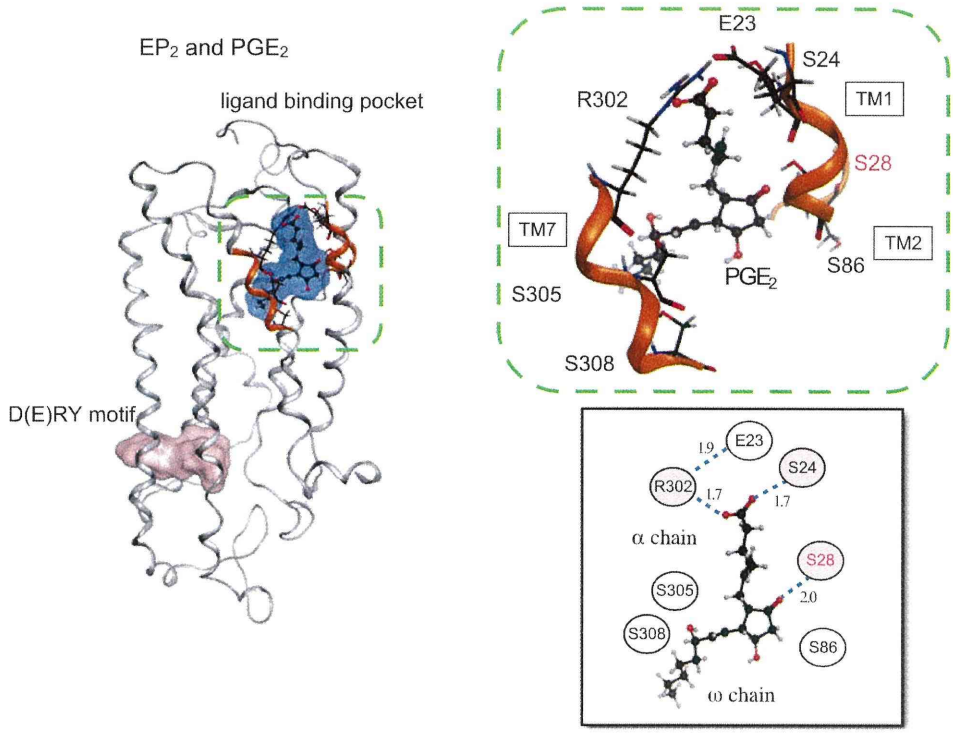

Fig. 4 Model structure of EP_2 with PGE_2. The whole and the local structures of EP_2 with PGE_2 are shown. The schematic diagram of the ligand–receptor interaction is also shown as an *inset*, where the average distances over the MD simulation (5–10 ns) between the ligand and the residues and those between the contact residue pairs are shown

PGE_2. These residues were mainly located on TM1, TM2, TM3, TM7, and ECL2. The side-chain of W186 (ECL2) and that of $Y93^{2.65}$ at the end of TM2 were directed toward the ligand-binding pocket, which may determine the ligand location. The cyclopentane ring of PGE_2 was surrounded by four Ser residues (Fig. 4). One of them, $S28^{1.39}$, is specifically conserved in EP_2 and formed a stable hydrogen bond with the carbonyl oxygen of the cyclopentane ring (see Supplement 7). The remaining three Ser residues did not directly interact with PGE_2. $S86^{2.58}$ existed near $S28^{1.39}$. This Ser was conserved not only within EP_2 but also within DP. The other two Ser residues, $S305^{7.43}$ and $S308^{7.46}$, existed on the opposite side of the cyclopentane ring against $S28^{1.39}$ and $S86^{2.58}$. The two residues were also conserved in both EP_2 and DP. The α chain of PGE_2 was extended toward the extracellular region. The hydrophobic environment around the α chain comprised $I27^{1.38}$, $M31^{1.42}$, $V89^{2.61}$, $Y93^{2.65}$, W186 (ECL2), and $L301^{7.39}$. The carboxy group at the terminus of the α chain interacted mainly with $R302^{7.40}$, as described above. In addition, $S24^{1.35}$ also interacted with the carboxy group. $R302^{7.40}$ constituted a network by forming salt bridges with $E23^{1.34}$. The network may contribute to determining both the relative arrangement of TM1 and TM7 and the location of the carboxy group of PGE_2 in the ligand-binding pocket. On the other hand, the ω chain was extended toward the middle of the membrane. The hydrophobic environment around the ω chain was composed of $L80^{2.52}$, $I85^{2.57}$, $M116^{3.32}$, $F119^{3.35}$, and W186 (ECL2). In the model structure, no amino acid residue that directly interacts with the hydroxy group in the ω chain was observed.

From the results of the sequence comparison and the analysis with CASTp, EP_2 had five specifically conserved residues, $S28^{1.39}$, $M31^{1.42}$, $T82^{2.54}$, $T123^{3.39}$, and $N307^{7.45}$, on the pocket surface. The MD simulation revealed the interaction between $S28^{1.39}$ and the carbonyl oxygen in the cyclopentane ring of PGE_2. In DP, the corresponding site was occupied by Gly, which is not expected to be involved in ligand recognition. However, three other PGE_2 receptors, EP_1, EP_3, and EP_4, have Pro at the corresponding site. On the other hand, no interaction was observed between the ligand and $M31^{1.42}$ or $T82^{2.54}$, although they were located close to PGE_2. $T123^{3.39}$ and $N307^{7.45}$ were farther from to the ligand. Therefore, the four specifically conserved residues are considered to be involved in some EP_2-specific function other than ligand recognition. In summary, several residues on TM1, TM2, and TM7 mainly contribute to the interaction with the ligand. Among them, $S28^{1.39}$, which may be involved in PGE_2-specific recognition, is located on TM1 of EP_2.

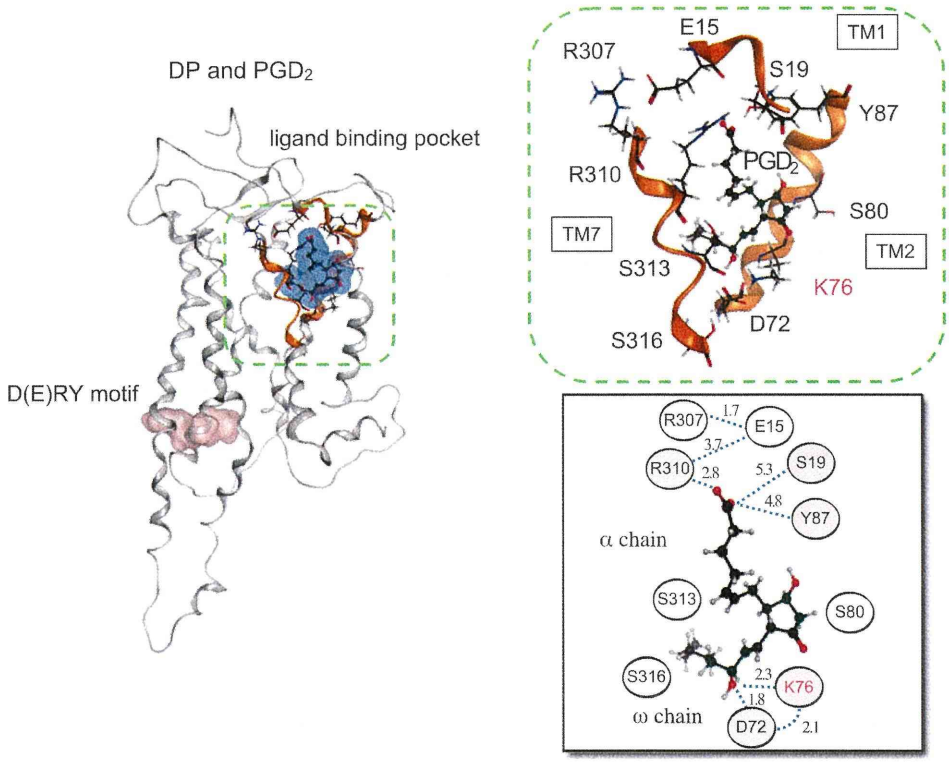

Fig. 5 Model structure of DP with PGD_2. The whole and the local structures of DP with PGD_2 are shown. The schematic diagram of the ligand–receptor interaction is also shown as an *inset*, where the average distances over the MD simulation (5–10 ns) between the ligand and the residues and those between the contact residue pairs are shown

3.2.3.2 Interaction between DP and PGD_2 As in the case of EP_2, 10 structures were sampled from the last 1 ns of the simulation of the ligand-bound model of DP. The MM-GBSA ligand interaction energies of these structures are shown in Supplement 9. In the DP model structure with the lowest MM-GBSA energy, 28 amino acid residues were found within 5 Å from PGD_2 (see Fig. 3). These residues were mainly located on TM1, TM2, TM3, and TM7. The ligand location seemed to be restricted by the bulky side chains of $Y87^{2.65}$, $F111^{3.31}$, $F115^{3.35}$, and W182 (ECL2). The whole structure and the vicinity of the ligand in the model with the lowest MM-GBSA energy are shown in Fig. 5. The hydrogen bonds between DP and PGD_2 described below were stable during the MD simulation (Supplement 7). The α chain was extended to the extracellular region, in a similar manner to those of PGE_2 in EP_2, and was surrounded by the hydrophobic residues $M22^{1.38}$, $L26^{1.42}$, $V83^{2.61}$, $L84^{2.62}$, $Y87^{2.65}$, $L306^{7.36}$, $L309^{7.39}$, and $V314^{7.44}$. The carboxy group at the terminus of the α chain interacted with $R310^{7.40}$. In addition, the carboxy group formed a hydrogen bond with $S19^{1.35}$ and $Y87^{2.65}$. $R307^{7.37}$ and $R310^{7.40}$ created an intramolecular salt bridge network with $E15^{1.31}$. As in the case of the ligand-bound EP_2 model structure, both the relative arrangement of TM1 and TM7 and the location of the carboxy group of PGD_2 in the ligand-binding pocket seemed to be determined by the intramolecular network. On the other hand, the ω chain was bent in the membrane and was surrounded by the hydrophobic residues, $L79^{2.57}$, $V83^{2.61}$, $F111^{3.31}$, $M112^{3.32}$, $F115^{3.35}$, $L117^{3.35}$, W182 (ECL2), $V281^{6.51}$, $L309^{7.39}$, $L312^{7.42}$, and $I315^{7.45}$. The hydroxy group in the ω chain interacted with $D72^{2.50}$ and $K76^{2.54}$, and these two residues also formed a salt bridge with each other (Supplement 7). No residue that interacted with the cyclopentane ring part was found during the simulation. Three Ser residues, $S80^{2.58}$, $S313^{7.43}$, and $S316^{7.46}$, were present in the middle of the membrane. $S313^{7.43}$ and $S316^{7.46}$ interacted with $K76^{2.54}$ (data not shown). These residues may contribute to the stabilization of the three oxygens of the cyclopentane ring and the ω chain by providing a hydrophilic environment, although there was no direct interaction between the serine residues and the oxygens. The three residues corresponded to the conserved Ser residues of EP_2, $S86^{2.58}$, $S305^{7.43}$, and $S308^{7.46}$.

According to the sequence comparison and the analysis with CASTp, eight residues were specifically conserved on the pocket surface in DP. Among them, $K76^{2.54}$ formed a

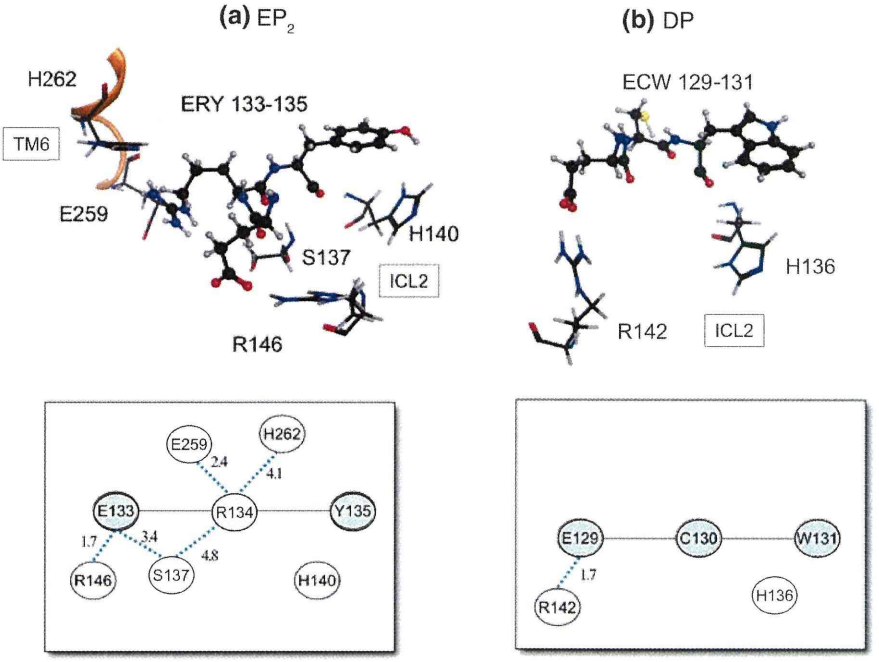

Fig. 6 The intramolecular interaction networks around the D(E)RY motif. The structures and the schematic diagrams for (**a**) EP_2 with PGE_2 and (**b**) DP with PGD_2 are shown. The average distances over the MD simulations (5–10 ns) between the contact residue pairs are shown in the schematic diagram

hydrogen bond with the hydroxy group in the ω chain. The Lys was experimentally suggested to be essential for ligand recognition [46]. On the one hand, a hydrogen bond between the Lys and the carbonyl oxygen of the cyclopentane ring was formed by an MD simulation [14]. However, in our simulation, this interaction was not observed. In EP_2, the corresponding site was occupied by the specifically conserved $T82^{2.54}$. This Thr did not interact with the ligand in the EP_2 model structure. Three other specifically conserved residues, $M22^{1.38}$, $G23^{1.39}$, and $L26^{1.42}$, were found near the ligand. $M22^{1.38}$ and $G23^{1.39}$ existed near the α chain, whereas $L26^{1.42}$ was close to the cyclopentane ring. However, the three residues did not interact with the ligand. The remaining four residues, S92 (ECL1), L104 (ECL1), $I282^{6.52}$, and $I315^{7.45}$, were not considered to be involved in the ligand recognition, since they were farther away from the ligand. As in the case of EP_2, TM1, TM2, and TM7 are also important for ligand recognition in DP. In contrast to the case of EP_2, $K76^{2.54}$ on TM2 may be involved in the ligand recognition.

3.3 Differences in intramolecular interactions around the D(E)RY motif between EP_2 and DP

As described above, the D(E)RY motif of GPCR is important for signal transduction [15]. The vicinity around the motif, Glu–Arg–Tyr (133–135), of the EP_2 model structure, is shown in Fig. 6a. $E133^{3.49}$ mainly interacted with R146 (ICL2) by forming a stable salt bridge and occasionally formed a hydrogen bond with S137 (ICL2). $R134^{3.50}$ formed a stable interaction with $E259^{6.40}$ and sometimes interacted with S137 (ICL2) during the MD (Supplement 7). $R134^{3.50}$ and $H262^{6.43}$ were located close to each other and may form a π-π interaction. The side chains of $E133^{3.49}$ and $R134^{3.50}$ were oriented in different directions, since they interact with other residues. H140 (ICL2) was present in the vicinity of $Y135^{3.51}$, the third residue of the motif. The side chains of the two residues were stacked upon one another, and the distance between them was about 5 Å. Therefore, the residues seemed to form a π–π interaction.

As described above, the D(E)RY motif of DP is mutated to Glu–Cys–Trp (129-131). The pattern of the intramolecular network around the motif in DP was quite different from that in EP_2. The interaction was only detected between $E129^{3.49}$ and R142 (ICL2) (Fig. 6b). The middle residue of the motif, $R134^{3.50}$ of EP_2, was substituted with Cys in DP. Due to the mutation, the interaction between the motif and TM6 was not observed in the DP model structure. H136 (ICL2), which corresponded to H140 (ICL2) of EP_2, was present near $W131^{3.51}$. The side chains were stacked upon one another, with a distance of about 6 Å.

4 Discussion

In this study, we have assumed that the amino acid residues specifically conserved in EP_2 and DP are related to the ligand recognition by the receptors. Our simulation study suggested that one of the specifically conserved residues in EP_2, $S28^{1.39}$, is involved in the recognition of the carbonyl oxygen of the cyclopentane ring. However, three other

PGE_2 receptors, EP_1, EP_3, and EP_4, have Pro at the corresponding site. As described above, the ancestor of the PNRs was considered to be the PGE_2 receptor. The observation of Pro in EP_1, EP_3, and EP_4 at the site suggests that the original residue in the ancestral PGE_2 receptor was Pro and that the ligand recognition mechanism of EP_2 may be different from those of the other PGE_2 receptors and the ancestral receptor, although they share PGE_2 as their ligand. DP lacks binding affinity to PGE_2 [47]. In DP, the residue corresponding to $S28^{1.39}$ is substituted with Gly. Our simulation study of DP suggested that the Gly residue is not involved in the recognition of PGD_2. Kobayashi et al. [46] generated a chimera between IP and DP, in which ICL1, TM2, and ECL1 were derived from IP to the remaining parts of the molecule were from DP. The chimera did not bind to either PGE_2 or PGD_2. When the Gly on TM1 in the DP region of the chimera was substituted with Ser, the mutant acquired the ability to bind PGE_2. The experiment seems to indirectly support the importance of the Ser residue for the recognition of PGE_2.

On the other hand, $K76^{2.54}$ was specifically conserved in DP. Our simulation study suggested that this residue is involved in the recognition of the hydroxy group of the ω chain of PGD_2. No residues interacted with either the hydroxy group or the carbonyl oxygen of the cyclopentane ring of PGD_2 in our simulation. In contrast, no residue that could interact with the hydroxy group of the ω chain of PGE_2 was detected in the simulation of EP_2. Therefore, the hydrogen bond formation between the hydroxy group and $K76^{2.54}$ may regulate the specific ligand recognition by DP. As described above, Li et al. [14] suggested that the Lys can form a hydrogen bond with the carbonyl oxygen in the cyclopentane ring of PGD_2, based on their MD simulation. Thus, our result is inconsistent with their report. However, the average distance between $K76^{2.54}$ and the carbonyl oxygen was 4.9 Å, and some rotamers of the residue were in a position that could interact with the oxygen (data not shown). Therefore, it is still possible that $K76^{2.54}$ also interacts with the carbonyl oxygen. For both PGE_2 and PGD_2, the α chain extended toward the outside of the receptors, whereas the cyclopentane ring and the ω chain extended between TM1 and TM2. The modification of the amino acid residues on the two helices is considered to have been effective to change the ligand recognition mechanism.

The D(E)RY motif is a conserved amino acid stretch in the cytoplasmic region of TM3. The cytoplasmic interaction network between the D(E)RY motif and TM6 is considered to be involved in the activation of the receptor. The network is called an "ionic lock", which is disrupted during the activation to release the constraints on the relative movement of TM3 and TM6 in some class A GPCRs, such as rhodpsin and β_2-adrenergic receptor [48]. The salt bridge between the first and second residues of the motif in the inactivated form is also observed [15]. EP_2 has the canonical D(E)RY motif. $E133^{3.49}$ of the motif did not form a salt bridge with the second residue of the motif, $R134^{3.50}$, but interacted with R146 (ICL2). $R134^{3.50}$ formed a salt bridge with $E259^{6.30}$. To examine the release of the ionic lock by the simulation study, more time steps may be required. In contrast to the canonical motif of EP_2, the D(E)RY motif of DP is mutated. The highly conserved Arg at the second position of the motif is substituted with Cys. Rosenkilde et al. [19] examined 365 human rhodopsin-like GPCRs and reported that only 3% lack the basic residue at this position. In our simulation study, the interaction between the motif and TM6 was absent in DP, due to the mutation. However, DP can exert its signal transduction activity. Therefore, DP may use a different mechanism for receptor activation, corresponding to the ionic lock. This hypothesis seemed to be consistent with the results of the experimental studies on other class A GPCRs. The D(E)RY motifs of various GPCRs have been subjected to amino acid substitution experiments to examine their functional meanings [49]. Such mutants are expected to be constitutively active, since they cannot form the ionic lock. Actually, some GPCR mutants are constitutively active. For example, FP becomes constitutively active by the mutation of the D(E)RY motif [50]. However, quite a few mutants are not constitutively active, such as the mutant of TP [51]. Both FP and TP have the canonical D(E)RY motif. As shown in Fig. 2, EP_2 and DP belong to one of the subtrees, whereas FP and TP are members of the other subtree. Therefore, it seems that the activation mechanism of PNRs may have rapidly diverged during evolution, and at least DP and TP acquired the activation mechanism without the ionic lock. Further experimental and computational studies are needed to solve this problem.

We have described a synergistic study integrating different computational approaches. The evolutionary information obtained from sequence comparisons is useful to select proper targets for computational studies and to identify the candidates of functionally important residues. Structural information obtained from homology modeling and docking analyses provides further clues to refine the candidate residues. Molecular dynamics simulations provided dynamic views for this study, which could not be obtained from static analyses with sequence comparisons and modeling. Thus, combining the information obtained from different computational approaches with that from the literature seems to be more efficient than using an individual approach, if the proper combination is adopted.

In this study, we used the PNRs as a concrete example for the application of the synergistic study. However, many questions about the PNRs still remain. For example, CRTH2 is known to function as a PGD_2 receptor [7], but

the evolutionary origin of the receptor differs from that of DP [8], as described above. Whether CRTH2 and DP share the same ligand recognition mechanism is an interesting subject, not only from a pharmaceutical viewpoint but also from an evolutionary perspective. A synergistic study may provide clues to address this issue. Computational analyses will accelerate the studies of PNRs.

Acknowledgments We thank Drs. Wataru Nemoto, Kentaro Tomii, and Makiko Suwa of CBRC for useful discussions on this work. HD was supported in part by the Global COE program, "an In Silico Medicine", at Osaka University and Grants-in-Aid (Nos. 20650012 and 19650072) from the Ministry of Education, Culture, Sports, Science and Technology of Japan. HT was partially supported by Targeted Proteins Research Program (TPRP).

References

1. Funk CD (2001) Science 294:1871–1875
2. Samuelsson B, Morgenstern R, Jakobsson PJ (2007) Pharmacol Rev 59:207–224
3. Wang MT, Honn KV, Nie D (2007) Cancer Metastasis Rev 26:525–534
4. Schuligoi R et al (2010) Pharmacology 85:372–382
5. Jones RL, Giembycz MA, Woodward DF (2009) Br J Pharmacol 158:104–145
6. Matsuoka T, Narumiya S (2007) Sci World J 7:1329–1347
7. Hirai H et al (2001) J Exp Med 193:255–261
8. Hata AN, Breyer RM (2004) Pharmacol Ther 103:147–166
9. Kedzie KM, Donello JE, Krauss HA, Regan JW, Gil DW (1998) Mol Pharmacol 54:584–590
10. Chang C, Negishi M, Nishigaki N, Ichikawa A (1997) Biochem J 322:597–601
11. Stitham J, Stojanovic A, Merenick BL, O'Hara KA, Hwa J (2002) J Biol Chem 278:4250–4257
12. Funk CD, Furci L, Moran N, Fitzgerald GA (1993) Mol Pharmacol 44:934–939
13. Neuschäfer-Rube F, Engemaier E, Koch S, Böer U, Püschel GP (2003) Biochem J 371:443–449
14. Li Y et al (2007) J Am Chem Soc 129:10720–10731
15. Rosenbaum DM, Rasmussen SG, Kobilka BK (2009) Nature 459:356–363
16. Scheer A, Fanelli F, Costa T, De Benedetti PG, Cotecchia S (1996) EMBO J 15:3566–3578
17. Wess J (1998) Pharmacol Ther 80:231–264
18. Ballesteros J, Palczewski K (2001) Curr Opin Drug Discov Devel 4:561–574
19. Rosenkilde MM, Kledal TN, Schwartz TW (2005) Mol Pharmacol 68:11–19
20. Lu ZL, Curtis CA, Jones PG, Pavia J, Hulme EC (1997) Mol Pharmacol 51:234–241
21. Altschul SF, Madden TL, Schäffer AA, Zhang J, Zhang Z, Miller W, Lipman DJ (1997) Nucleic Acids Res 25:3389–3402
22. Ballesteros JA, Weinstein H (1995) Methods Neurosci 25:366–428
23. Katoh K, Misawa K, Kuma K, Miyata T (2002) Nucleic Acids Res 30:3059–3066
24. Katoh K, Toh H (2008) Brief Bioinform 9:286–298
25. Saitou N, Nei M (1987) Mol Biol Evol 4:406–425
26. Felsenstein J (1996) Methods Enzymol 266:418–427
27. Jones DT, Taylor WR, Thornton JM (1992) Comput Appl Biosci 8:275–282
28. Felsenstein J (1985) Evolution 39:783–791
29. Felsenstein J (1993) PHYLIP (phylogeny inference package), version 3.5c. University of Washington, Seattle
30. Adachi J, Hasegawa M (1996) MOLPHY (programs for molecular phylogenetics), version 2.3b3. Institute of Statistical Mathematics, Tokyo
31. Halgren TA (1996) J Comput Chem 17:490–519
32. Labute P (2008) J Comput Chem 29:1693–1698
33. Wiederstein M, Sippl MJ (2007) Nucleic Acids Res 35:W407–W410
34. Sippl MJ (1993) Proteins 17:355–362
35. Goto J, Kataoka R (2008) J Chem Inf Model 48:583–590
36. Bowers KJ, Chow E, Xu H, Dror RO, Eastwood MP, Gregersen BA, Klepeis JL, Kolossvary I, Moraes MA, Sacerdoti FD, Salmon JK, Shan Y, Shaw DE (2006) In: Proceedings of the ACM/IEEE conference on Supercomputing, Tampa, November 11-17, ACM New York, USA. doi:10.1145/1188455.1188544
37. Banks JL, Beard HS, Cao Y, Cho AE, Damm W, Farid B, Felts AK, Halgren TA, Mainz DT, Maple JR, Murphy R, Philipp DM, Repasky MP, Zhang LY, Berne BJ, Friesner RA, Gallicchio E, Levy RM (2005) J Comput Chem 26:1752–1780
38. Krautler V (2001) J Comput Chem 22:501–508
39. Darden T, York D, Pedersen L (1993) J Chem Phys 98:10089–10092
40. Lyne PD, Lamb M, Saeh JC (2006) J Med Chem 49:4805–4808
41. Toh H, Ichikawa A, Narumiya S (1995) FEBS Lett 361:17–21
42. Fritze O et al (2003) Proc Natl Acad Sci USA 100:2290–2295
43. Paila YD, Tiwari S, Chattopadhyay A (2008) Biochim Biophys Acta 1788:295–302
44. Dundas J, Ouyang Z, Tseng J, Binkowski A, Turpaz Y, Liang J (2006) Nucleic Acids Res 34:W116–W118
45. Jaakola V-P, Prilusky J, Sussman JL, Goldman A (2005) Protein Eng Des Sel 18:103–110
46. Kobayashi T, Ushikubi F, Narumiya S (2000) J Biol Chem 275:24294–24303
47. Tsuboi K, Sugimoto Y, Ichikawa A (2002) Prostaglandins Other Lipid Mediat 68–69:535–556
48. Vogel R, Mahalingam M, Lüdeke S, Huber T, Siebert F, Sakmar TP (2008) J Mol Biol 380:648–655
49. Rovati GE, Capra V, Neubig RR (2007) Mol Pharmacol 71:959–964
50. Pathe-Neuschäfer-Rube A, Neuschäfer-Rube F, Püschel GP (2005) Biochem J 388:317–324
51. Ambrosio M, Fanelli F, Brocchetti S, Raimondi F, Mauri M, Rovati GE, Capra V (2010) Cell Mol Life Sci 67:2979–2989
52. Tusnády GE, Dosztányi Z, Simon I (2005) Bioinformatics 21:1276–1277

Microbiology and Immunology

Microbiol Immunol 2012; **56**: 99–106
doi:10.1111/j.1348-0421.2012.00412.x

ORIGINAL ARTICLE

Reactivity of human convalescent sera with influenza virus hemagglutinin protein mutants at antigenic site A

Eri Nobusawa, Katsumi Omagari, Setsuko Nakajima and Katsuhisa Nakajima

Department of Virology, Nagoya City University Graduate School of Medical Science, Nagoya City, Aichi, Japan

ABSTRACT

How the antibodies of individual convalescent human sera bind to each amino acid residue at the antigenic sites of hemagglutinin (HA) of influenza viruses, and how the antigenic drift strains of influenza viruses are selected by human sera, is not well understood. In our previous study, it was found by a binding assay with a chimeric HA between A/Kamata/14/91 (Ka/91) and A/Aichi/2/68 that convalescent human sera, following Ka/91 like (H3N2) virus infection, bind to antigenic site A of Ka/91 HA. Here using chimeric HAs possessing single amino acid substitutions at site A, it was determined how those human sera recognize each amino acid residue at antigenic site A. It was found that the capacity of human sera to recognize amino acid substitutions at site A differs from one person to another and that some amino acid substitutions result in all convalescent human sera losing their binding capacity. Among these amino acid substitutions, certain ones might be selected by chance, thus creating successive antigenic drift. Phylogenetic analysis of the drift strains of Ka/91 showed amino acid substitutions at positions 133, 135 and 145 were on the main stream of the phylogenetic tree. Indeed, all of the investigated convalescent sera failed to recognize one of them.

Key words antigenic drift, hemagglutinin, human sera.

Influenza is an acute infectious respiratory disease caused by influenza viruses. To date, vaccines have failed to control influenza and epidemics occur every winter season. Influenza virus has a remarkable ability to escape host defense mechanisms by altering the antigenic character of its HA and NA proteins, especially through changes in amino acid residues on the HA molecule. In order to find ways to control influenza epidemics, it is important to elucidate the molecular mechanisms by which viruses alter their antigenic character and thus escape from human anti-sera. Analyses of natural and laboratory-selected antigenic variants have resulted in identification of four to five antigenic sites on the HA protein of influenza A (H3N2) viruses (1–3).

Longstanding observations have demonstrated the role of serum antibodies to HA protein in protecting against infection (4–6). Serum antibodies are also important in recovery from influenza virus infection (7–9). The specificity with which human serum antibodies bind to antigenic sites on the HA protein varies considerably from person to person (10, 11), suggesting that antigenic variants may arise in individuals who are only partially immunized (i.e. who have not developed antibodies to all antigenic sites) and are susceptible to mutants in which only one or two antigenic sites have been changed (12). The question is how, under immune pressure, are the amino acid substitutions that distinguish drift strains from the original strain selected.

Correspondence
Eri Nobusawa, Influenza Virus Research Center, National Institute of Infectious Diseases, 4–7–1, Gakuen, Musashi Murayama-shi, Tokyo, 208–0011, Japan.
Tel: +81 42 848 7168; fax: +81 42 561 6124; email: nobusawa@nih.go.jp

Received 3 August 2011; revised 5 December 2011; accepted 8 December 2011.

List of Abbreviations: Ai, Aichi; HA, hemagglutinin; HI, hemagglutination inhibition; Ka, Kamata; mAb, monoclonal antibody; MEM, minimal essential medium; NA, neuraminidase; NI, neutralization inhibition; S1, acute phase; S2, convalescent phase.

Researchers have reported that distinct mAbs with different amino acid sequences can recognize the same epitopes on an antigen molecule (6, 13). In their study of anti-HA antibodies, Fleury *et al.* (13) showed that binding of HC45 Fab and BH151 Fab has very similar orientations and positions with regard to the molecule of A/Aichi/2/68 (Ai/68) and displays a similar affinity, but that HC45 interacts with many more amino acid residues on the HA molecule. In experiments with anti-NA antibodies, Malby *et al.* (14) showed that NC10 and NC41 make contact with the NA molecule through a common set of residues but most of the interactions with these residues differ sterically and chemically between the two complexes.

Even when they are raised against a similar antigen and recognize the same antigenic site, the amino acid sequences of the antigen binding-region on neutralizing antibodies may differ from person to person. Therefore, at the antigenic sites of HA, amino acid residues that interact with individual neutralizing antibodies may also vary from person to person. If individual antibodies recognize the corresponding antigenic sites differently, how are particular amino acid substitutions selected under immune pressures, causing antigenic drift?

We previously reported that a chimeric HA protein method can be used to determine the capacity of human sera to bind to each antigenic site (11) and also showed that semi-quantitative binding of human sera to H3HA correlates with HI activity (16). In that study, we examined the ability of paired sera obtained from eight patients aged 3 to 14 years, who were infected with influenza A (H3N2) virus during 1990–1991, to bind to chimeric HA proteins expressed on COS cells by an expression vector. Individual convalescent sera bound to different antigenic regions of A/Kamata/14/91 (H3N2)(Ka/91) HA: site C/E, site A, site A/B1, site B2 and site C, depending on the patient's age. Recently we analyzed escape mutants selected with mAb203 raised against Ka/91, and found that the amino acid residues at nine positions of antigenic site A of mutants differed from those found in Ka/91 HA (17). To understand how the character of the amino acid residues constituting the epitope affects binding to mAb203, we introduced one-point amino acid substitutions into those nine positions of Ka/91 HA and analyzed their binding to mAb203. We showed that the ability of mAb203 to bind to mutant HA molecules depends on the positions and species of substituted amino acid residues. To extend our knowledge of antigenic drift, in the present study we attempted to discern amino acid substitutions in HA related to antigenic drift of Ka/91. All the convalescent sera used in our previous study showed decreased HI reactivity with drift strains of Ka/91 and five of the convalescent sera bound to site A of Ka/91 HA (11). In regard to the effect of the mutations at site A on the mAb203 binding, we analyzed the binding capacity of those convalescent sera to mutant HAs with one-point mutations at site A similar to those found in the previous study.

MATERIALS AND METHODS

Human sera

Paired sera from four patients aged 12 to 14 years who were infected with influenza A (H3N2) viruses during January to February in 1991 were used (11). The sera of the acute and convalescent phase were collected two to three days and two to three months after the onset of the fever, respectively. The convalescent sera bound only to the chimeric HA Ka91/Ai68, which includes the HA1 region of Ka/91 and the HA2 region of Ai/68, but not to the chimeric HA, Ai68/Ka91, which includes the HA1 region of Ai/68 and the HA2 region of Ka/91(11).

Mouse monoclonal antibodies

Mouse mAbs 203 and 35 directed against the HA protein of Ka/91 were obtained as described previously (11).

Chimeric hemagglutinin cDNAs

cDNA of chimeric HA, #2HA, in which amino acid residues between positions 96 and 150 of Ai/68 HA had been replaced with those of Ka/91 HA (Fig. 1), was cloned into an expression vector pME18s (pME18s-#2HA) as described previously (11).

Site-directed mutagenesis

Site-directed mutations were introduced between amino acid residues at positions 96 to 150 of #2HA using the Mutan-Super Express Km kit (Takara Bio, Shiga, Japan) as follows. Briefly, the PCR product of pME18s-#2HA DNA amplified with primers pME (−) (18) and KO2 (19) was digested with EcoRI and PstI. The EcoRI/PstI fragment was inserted into pKF18k (pKF18k-#2HA) and the desired clones were obtained in JM103 in the presence of kanamycin (0.17 μg/mL). The PCR product of pKf18k-#2HA DNA (8 p mol) amplified with a selection primer (Takara Bio) and a mutant primer was precipitated with NH4-acetate and ethanol, and then dissolved in water. The PCR products were then cloned in MV1184 in the presence of kanamycin (1 μg/mL). Selected mutant cDNAs were digested with EcoRI and NdeI. These fragments were then replaced with the counterpart of #2HA cDNA.

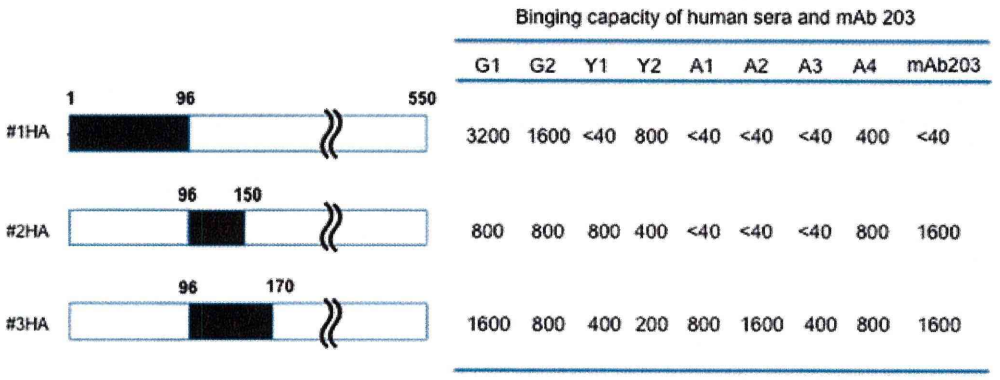

Fig. 1. Binding capacity of each patient's convalescent serum and mAb203 to chimeric HA proteins, #1HA to #3HA. Chimeric HAs expressed on Cos cells were stained with diluted sera and FITC-labeled anti-human goat serum. The binding capacity of the convalescent sera of each patient, G1, G2, Y1, Y2, A1, A2, A3, and A4, was expressed as the highest dilution point at which the expressed HAs were detected by the diluted sera. This figure is prepared partially based on data from a previous study (11).

Immunofluorescent staining of the hemagglutinin protein expressed in COS cells

Transfection was performed as described previously (19, 15). Briefly, each cDNA (200 ng) in MEM was incubated with lipofectamine for 15 min at room temperature. COS cells (0.5×10^5 cells/18 mm coverglass) prepared 18 hr before use were washed with MEM. The DNA and lipofectamine mixture was added to the cells, which were then incubated for 6 hr at 37°C. The medium was changed to MEM containing 10% FCS and the cells were further incubated for 42 hr at 37°C. The cells were then fixed with ethanol–acetone (1:1) at 4 C for 15 min. Indirect immunofluorescent staining was performed with human sera, mouse mAb203 or 35 and FITC-labeled anti-human or anti-mouse goat anti-sera. mAb35, which recognize both the Ka/91and Ai/68 HA proteins, was used to confirm expression of #2HA and mutant HA in the COS cells. For the quantitative FITC assay using diluted human sera, two separate experiments were carried out. The difference in values was not more than twofold and the smaller of the two values was used as described previously (11, 16).

Three-dimensional modeling

To construct a model of the HA protein of Ka/91, the structure of Ai/68 (1HGF.pdb, Protein Data Bank) was modified. Amino acids of Ai/68 were replaced one by one according to the evolution of H3HA until they were the same as those of Ka/91 and the model constructed using CAChe version 6.1 software (Fujitsu, Japan) with the MM2 calculation program. Optimization continued until the energy change became less than 0.001 kcal/mol as described previously (17). The model structure of chimerical #2HA was also constructed using the method described above.

RESULTS

Characteristics of convalescent human sera and mAb203 raised against Ka/91

In our previous study, we investigated the binding properties to Ka/91-HA of eight paired sera collected during S1 and S2 from patients infected with Ka/91-like viruses during influenza season 1991/1992 (11). In brief, we created chimeric HAs by connecting Ka/91(black) and Ai/68 (white) HA at the indicated positions of the amino acid sequence numbers (Fig. 1). #1HA includes parts of antigenic site C and E of Ka/91HA. #2HA and #3HA include antigenic site A, and antigenic sites A and B1 of Ka/91HA, respectively. We stained each chimeric HA expressed on COS cells with serially diluted patient sera and FITC-labeled anti-human goat serum; the binding capacity of antibodies in the sera to the other antigenic sites of KA/91-HA could be disregarded. We found the convalescent sera of four patients (G1, G2 Y2, and A4), five patients (G1, G2, Y1, Y2 and A4), and all patients bound to the antigenic site(s) C/E, A, and A/B1, respectively (Fig. 1).

In this study, we used G1, G2, Y1 and Y2 sera to investigate the influence of amino acid substitutions at site A of Ka/91-HA on the binding capacity of human sera. We introduced the following one-point amino acid substitutions into the antigenic site A of the chimeric #2HA: A131D, A131T, G142E, G142R, G142V, G142S, S143P, V144I and S146N.

Amino acid substitutions in the HA1 region of Ka/91 occur at 14% of the HA1 positions in Ai/68. Therefore,

the fine structures of these two HAs might be different. We used molecular mechanics calculations to model the structure of Ka/91 and chimeric #2HA based on the Ai/68-HA structure (Fig. 2). The modeled structures of their antigenic site A were not so different from that of Ai/68-HA. Amino acid residues from Ka/91 (yellow), including site A (green) and mutated positions (red and purple) are indicated on the structure of chimeric #2HA.

Differences in the binding properties of mAb203 to chimeric #2HA mutants carrying one-point amino acid substitutions at site A depend on the character of the substituted amino acid residues. There are negative mutations, A131D, A131T, G142E, G142R, G142V, G142S, and S143P, and positive mutations, V144I and S146N. The former were not recognized. However, the latter were recognized by mAb203, which is the same result as that of our previous study using full Ka/91-HA (17).

The binding properties of human convalescent sera to amino acid residues at site A on the H3HA protein

We confirmed the extent of expression of mutant HA on COS cells by indirect immunofluorescent staining using mAb35, which recognizes both Ka/91 and Ai/68 HA. We stained all mutant HAs by mAb35 diluted 3200- to 6400-fold. We performed semi-quantitative analysis of the binding capacity by determining the limiting dilution for each human convalescent serum by indirect immunofluorescent staining. All human sera bound to chimeric #2HA equally with a binding capacity up to 1:800. However, their binding capacity to each mutant HA differed from person to person according to the character and positions of the substituted amino acid residues (Table 1), that is, G1, G2, and Y1 exhibited a binding capacity to A131D up to a dilution of 1:400 to 1:800, but Y2 and mAb203 did not. As for amino acid substitutions at position 142, the binding capacity of G1 to the mutant HAs depended on the substituted amino acid residues, but that of Y1 and Y2 to mutant HAs decreased regardless of the substituted amino acids. Similar to the reactivity of mAb203, all sera lost or decreased their binding capacity to mutant HAs with A131T and G142E (Table 1). This observation suggests that amino acid substitutions to which most sera lose their binding ability might be selected among field strains.

Hemagglutination inhibition reactivity of human sera and mAb203 to field strains

A summary of results of assessing the reactivity of human sera to field strains by the HI test is shown in Table 2. Only the convalescent sera reacted with Ka/91, A/Chiba/54/92, and A/Aichi/12/92 viruses but they did not react with the drift strains of Ka/91, A/Aichi/4/93, A/Aichi/48/93 and A/Aichi/2/94 viruses. As shown in Table 2, mAb203 also had reduced reactivity to these drift strains. Since these human sera and mAb203 bind to site A, the amino acid changes at site A on HA of the drift strains are responsible for the reduced reactivity.

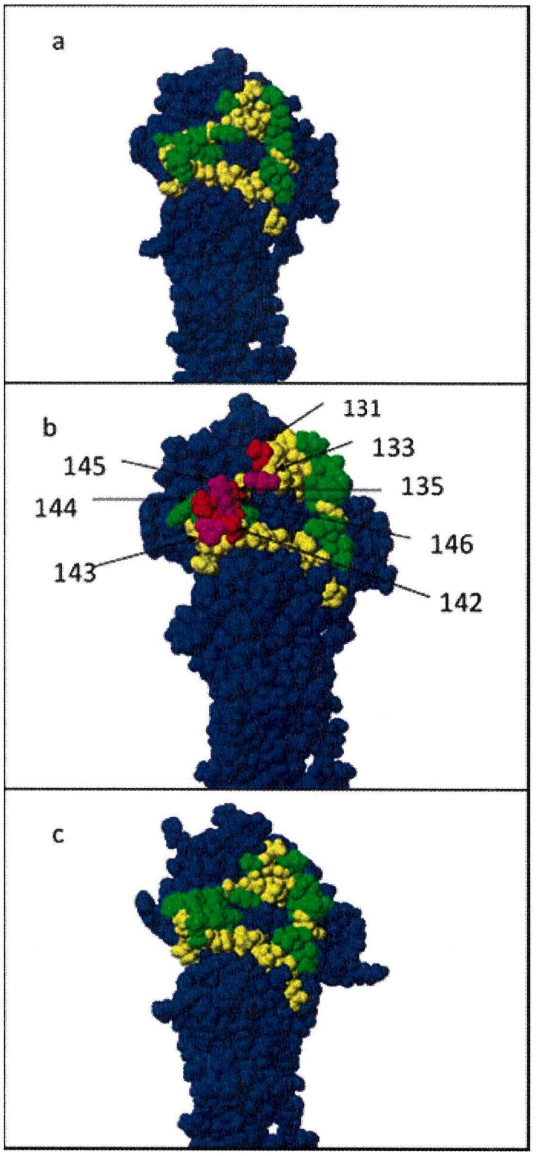

Fig. 2. Three-dimensional structure of HA models, (a) Ai/68 HA, (b) chimeric #2HA, and (c) Ka/91 HA. Three-dimensional HA models of Ka/91 and #2HA were constructed using a molecular mechanics calculation method as described in Materials and Methods. The chimeric structure was constructed by replacement of residues 96–150 (yellow) including site A (green) of Ai68 with those of Ka91 using CAChe software (version 6.1) with the MM2 calculation program. The positions of the one-point mutations are shown in red and purple.

Table 1. Comparison of the binding capacity of each human convalescent serum and monoclonal antibodies to mutant HA

Mutant HAs† with amino acid changes	Human convalescent sera				Monoclonal antibodies	
	G1	G2	Y1	Y2	203	35
#2HA‡	800	800	800	800	3200	6400
A131D	800	800	400	100	<100	3200
A131T	<50	<50	<50	100	<100	1600
G142E	100	<50	<50	<50	<100	1600
G142R	800	800	<100	<100	<100	3200
G142V	200	200	100	<100	<100	6400
G142S	1600	200	200	200	<100	6400
S143P	800	<100	<100	<100	100	6400
V144I	1600	<100	800	200	1600	6400
S146N	800	<100	400	<100	400	6400
S133D§	800	400	800	<100	1600	6400
D135G§	800	400	400	400	1600	3200
K145N§	100	<100	200	<100	100	3200

†, chimeric #2 HA with one-point amino acid changes that were found in drift strains or escape mutants from mAb203; ‡, chimeric #2HA without mutations; §, the same mutation was found in the drift strains of Ka/91 virus.

Table 2. HI titers of patient sera and monoclonal antibody 203 (mAb203) against natural isolates (H3N2) between 1990 and 1994

Sera†	Age (years)	Natural isolates					
		Kamata/14/91	Aichi/12/92	Chiba/54/92	Aichi/4/93	Aichi/48/93	Aichi/2/94
G1-S1	14	20	20	20	20	20	20
G1-S2		320	320	320	40	40	40
G2-S1	12	20	20	20	20	20	20
G2-S2		320	320	320	80	80	80
Y1-S1	12	20	20	20	20	20	20
Y1-S2		160	160	160	20	20	20
Y2-S1	12	20	20	20	20	20	20
Y2-S2		160	160	160	40	40	40
mAb203		6400	NT	6400	<100	<100	<100

†, human sera of S1 and S2 after A/Kamata/14/91 infection. None of these patients had a history of vaccination. NT = Not tested.

Comparison of the amino acid sequences of field isolates collected during 1991 to 1994 seasons

In order to identify the amino acid substitutions responsible for the reduction of HI ability of human sera to the HA of A/Aichi/4/93, A/Aichi/48/93 and A/Aichi/2/94 viruses, we compared the amino acid sequences of the site A region between these three viruses' HAs and Ka/91 HA. Amino acid differences were found at positions 133, 135 and 145 (Fig. 3). To investigate the role of these amino acid changes in the antigenic drift of Ka/91 virus, we examined the phylogenetic relationships among the HAs of 36 natural isolates collected between 1991 and 1994 (sequences of the HA proteins were randomly selected from an influenza sequence data bank) by comparing the amino acid sequences of site A. The viruses were divided into two distinct groups, I and II (Fig. 4), which are distinguished from each other by their respective amino acid substitutions at positions 133(S to D)(S133D), 135(D/E to G/K), and 145(K to N)(K145N) of site A. The antigenic difference at site A on HA between group I and group II viruses may depend on the amino acid changes at these positions.

The amino acid changes responsible for antigenic drift of Ka/91 virus

To study the relationship between amino acid changes found in drift strains and the reduced HI reactivity of human sera and mAb203 with these strains, we further investigated the binding capacity of human convalescent sera to #2HA mutants with one-point amino acid substitutions S133D, D135G or K145N (Table 1). All sera but

```
          96                                                        150
Kamata14  NCYPYDVPDYASLRSLVASSGTLEFINEDFNWTGVAQSGDSYACKRGSVKSFFSR
Chiba54   ..........................T.............E..............
Aichi12   ..........................T.............E..............
Aichi4    ....................................D.G.........N.....
Aichi48   ....................................D.K.........N.....
Aichi2    ....................................D.K....R....N.....
          ************************.*********** * ****.**** *****
```

Fig. 3. Comparison of amino acid sequences between positions 96 and 150 of HA among field isolates. Amino acid sequences of Ka91-like viruses and its drift strains are aligned as follows: Ka91 (Kamata14), A/Chiba/54/92 (Chiba54), A/Aichi/12/92 (Aichi12), A/Aichi/4/93 (Aichi4), A/Aichi/48/93 (Aichi48), and A/Aichi/12/92 (Aichi12) viruses.

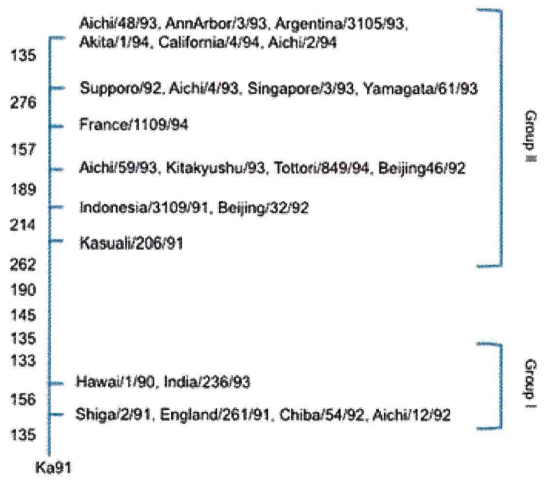

Fig. 4. Phylogenetic relationships among human H3N2 influenza viruses isolated from 1991 through 1994. The numbers on the mainstream designate the positions where we observed amino acid differences compared to Ka91. We divided the viruses into two distinct groups, group I and group II, according to their amino acid sequences.

Y2 bound to the mutant HAs with S133D and D135G. On the other hand, all sera showed lost/decreased binding to mutant HA with K145N (Table 1). mAb203 bound to the mutant HAs with S133D and D135G, but not to mutant HA with K145N.

DISCUSSION

Human serum is polyclonal, containing a mixture of antibodies that recognize different antigenic sites. The binding abilities of human sera used in the current experiments have already been reported in terms of their binding to sites C/E, A and B1 (G1, G2, and Y2), and sites A and B1 (Y1) (11). In addition, the present study showed that these anti-HA sera had different binding capacities to each mutant HA possessing an amino acid substitution at site A of Ka/91 HA. However, it is difficult to say whether the sera used in the present experiments consisted of mixed antibodies or of one main antibody reacting with site A. In any case, anti-HA antibodies induced in human sera by infection with Ka/91-like virus had different binding capacities to Ka/91 HA with substituted amino acid residues at site A.

In these experiments, because escape mutants from mAb203 contain amino acid substitutions only in the A2 and A3 subsites, and because amino acid differences at site A on the HA proteins of group I and II viruses have been observed only in A2 and A3, we introduced amino acid substitutions into the A2 (at positions 133–137) and A3 (at positions 142–147) subsites, but not into the A1 (at positions 121–126) subsite. As shown in Table 1, each human serum had a different binding capacity against each mutant HA with a substituted amino acid at site A on Ka/91 HA.

The different responses of each of the human antibodies to each amino acid substitution may depend on the particular characteristics of the antibody in regard to recognizing its own epitope. The antigenic change found at site A of group II viruses depends mainly on the amino acid substitution K145N. Additional changes at 133 and 135 may strengthen the likelihood of escape. Several authors have shown that, in antigenic drift, amino acid changes at more than two residues on the same antigenic site are common (20, 12). Referring to another antigenic site, in our previous study we happened to find that the amino acid change E156K at site B1 of chimeric #3HA reduced the binding ability of three patient sera to mutant HA. We found this amino acid change in several drift strains of Ka/91. Therefore, another amino acid change, E156K might also relate to antigenic drift of Ka/91. Clarification of the mechanism of antigenic drift by studying these chimeric HA with amino acid mutations and comprehensively analyzing many human convalescent sera for their

reactivities with all antigenic sites or mutant HA, and the breadth of responses to these, is yet to be undertaken.

Can the reason for selection of K145N among various natural isolates be determined? Amino acid substitutions A131T and G142E reduce the binding capacity of each human serum to a similar or greater extent than K145N. K145N occurred due to a transversional change in the genetic code from aaa to aac while A131T is due to a transitional change from gct to act. Arnold and Cameron have reported that RNA polymerase does not have a proofreading mechanism and has different frequencies of transition and transversion (21). *In vitro*, among the escape mutants from monoclonal antibodies against Ka/91 the number of transitional substitutions is reportedly double that of transversional ones (17). Regarding K145N, we expected amino acid substitutions to be selected by chance from the several restricted amino acid substitutions, regardless of the base substitutions in the corresponding codons.

In considering the escape of antigenic variants from human sera, we should take into account the neutralizing activity of each human serum. The different binding activities of each serum may correlate with differences in their HI reactivity because: (i) the sera used showed HI reactivity with Ka/91 virus (11); and (ii) semi-quantitative values of human sera in regard to binding to the HA1 region do correlate with HI titers (16).

Group I viruses may have played a major role in 1991 epidemics but they gradually decreased in importance in the 1992 and 1993 influenza seasons, group II viruses becoming the major strains at that time. Pressure from antisera may explain these phenomena. Human sera from group I virus-infected individuals barely neutralized group II viruses (Table 2); therefore, the latter strains may have been selected by antisera against group I viruses. In this report, we suggest that anti-HA antibodies differ from person to person and the response of an antibody to an amino acid substitution at antigenic sites also varies among individuals. Some amino acid substitutions caused all convalescent human sera to lose their binding capacity. We suspect that amino acid substitutions for successive antigenic drift were selected by chance from these several restricted amino acid substitutions.

ACKNOWLEDGMENTS

We are greatly indebted to J. Mosher for critical editing of the manuscript. We thank K. Maruyama for generously providing the pME18S expression vector. Finally, we are grateful to H. Kojima for her excellent technical assistance. This work was partially supported by a Health and Labor Sciences Research Grants from the Ministry of Health, Labor and Welfare of Japan.

DISCLOSURE

No authors have any conflicts of interest to disclose.

REFERENCES

1. Webster R.G., Laver W.G. (1980) Determination of the number of nonoverlapping antigenic areas on Hong Kong (H3N2) influenza virus hemagglutinin with monoclonal antibodies and the selection of variants with potential epidemiological significance. *Virology* **104**: 139–48.
2. Wiley D.C., Wilson I.A., Skehel J.J. (1981) Structural identification of the antibody-binding sites of Hong Kong influenza haemagglutinin and their involvement in antigenic variation. *Nature* **289**: 373–8.
3. Underwood P.A. (1982) Mapping of antigenic changes in the haemagglutinin of Hong Kong influenza (H3N2) strains using a large panel of monoclonal antibodies. *J Gen Virol* **62**:(Pt 1): 153–69.
4. Couch R.B., Kasel J.A. (1983) Immunity to influenza in man. *Annu Rev Microbiol* **37**: 529–49.
5. Dowdle W.R., Coleman M.T., Mostow S.R., Kaye H.S., Schoenbaum, S.C. (1973) Inactivated influenza vaccines. 2. Laboratory indices of protection. *Postgrad Med J* **49**: 159–63.
6. Hobson D., Curry R.L., Beare A.S., Ward-Gardner A. (1972) The role of serum haemagglutination-inhibiting antibody in protection against challenge infection with influenza A2 and B viruses. *J Hyg (Lond)* **70**: 767–77.
7. Epstein S.L., Misplon J.A., Lawson C.M., Subbarao E.K., Connors M., Murphy B.R. (1993) Beta 2-microglobulin-deficient mice can be protected against influenza A infection by vaccination with vaccinia-influenza recombinants expressing hemagglutinin and neuraminidase. *J Immunol* **150**: 5484–93.
8. Gerhard W., Mozdzanowska K., Furchner M., Washko G., Maiese, K. (1997) Role of the B-cell response in recovery of mice from primary influenza virus infection. *Immunol Rev* **159**: 95–103.
9. Palladino G., Mozdzanowska K., Washko G., Gerhard W. (1995) Virus-neutralizing antibodies of immunoglobulin G (IgG) but not of IgM or IgA isotypes can cure influenza virus pneumonia in SCID mice. *J Virol* **69**: 2075–81.
10. Wang M.L., Skehel J.J., Wiley D.C. (1986) Comparative analyses of the specificities of anti-influenza hemagglutinin antibodies in human sera. *J Virol* **57**: 124–8.
11. Nakajima S., Nobusawa E., Nakajima K. (2000) Variation in response among individuals to antigenic sites on the HA protein of human influenza virus may be responsible for the emergence of drift strains in the human population. *Virology* **274**: 220–31.
12. Wilson I.A., Cox N.J. (1990) Structural basis of immune recognition of influenza virus hemagglutinin. *Annu Rev Immunol* **8**: 737–71.
13. Fleury D., Daniels R.S., Skehel J.J., Knossow M., Bizebard T. (2000) Structural evidence for recognition of a single epitope by two distinct antibodies. *Proteins* **40**: 572–8.
14. Malby R.L., Tulip W.R., Harley V.R., Mckimm-Breschkin J.L., Laver W.G., Webster R.G., Colman P.M. (1994) The structure of a complex between the NC10 antibody and influenza virus neuraminidase and comparison with the overlapping binding site of the NC41 antibody. *Structure* **2**: 733–46.
15. Nobusawa E., Ishihara H., Morishita T., Sato K., Nakajima K. (2000) Change in receptor-binding specificity of recent human influenza A viruses (H3N2): a single amino acid change in hemagglutinin altered its recognition of sialyloligosaccharides. *Virology* **278**: 587–96.
16. Sato K., Morishita T., Nobusawa E., Tonegawa K., Sakae K., Nakajima S., Nakajima K. (2004) Amino-acid change on the

antigenic region B1 of H3 haemagglutinin may be a trigger for the emergence of drift strain of influenza. *A virus J Epidemiol Infect* **132**: 399–406.
17. Nakajima S., Nakajima K., Nobusawa E., Zhao J., Tanaka S., Fukuzawa K. (2007) Comparison of epitope structures of H3HAs through protein modeling of influenza A virus hemagglutinin: mechanism for selection of antigenic variants in the presence of a monoclonal antibody. *Microbiol Immunol* **51**: 1179–87.
18. Nakajima K., Nobusawa E., Tonegawa K., Nakajima S. (2003) Restriction of amino acid change in influenza A virus H3HA: comparison of amino acid changes observed in nature and in vitro. *J Virol* **77**: 10088–98.
19. Nakajima K., Nobusawa E., Nagy A., Nakajima, S. (2005) Accumulation of amino acid substitutions promotes irreversible structural changes in the hemagglutinin of human influenza AH3 virus during evolution. *J Virol* **79**: 6472–7.
20. Plotkin J.B., Dushoff J., Levin S.A. (2002) Hemagglutinin sequence clusters and the antigenic evolution of influenza A virus. *Proc Natl Acad Sci U S A* **99**: 6263–8.
21. Arnold J.J., Cameron C.E. (2004) Poliovirus RNA-dependent RNA polymerase (3Dpol): pre-steady-state kinetic analysis of ribonucleotide incorporation in the presence of Mg2+. *Biochemistry* **43**: 5126–37.

Theor Chem Acc (2011) 130:1197–1202
DOI 10.1007/s00214-011-1048-z

REGULAR ARTICLE

Antigen–antibody interactions of influenza virus hemagglutinin revealed by the fragment molecular orbital calculation

Akio Yoshioka · Kazutomo Takematsu · Ikuo Kurisaki · Kaori Fukuzawa · Yuji Mochizuki · Tatsuya Nakano · Eri Nobusawa · Katsuhisa Nakajima · Shigenori Tanaka

Received: 12 May 2011 / Accepted: 16 September 2011 / Published online: 4 October 2011

Abstract Effective interactions between amino acid residues in antigen–antibody complex of influenza virus hemagglutinin (HA) protein can be evaluated in terms of the inter-fragment interaction energy (IFIE) analysis with the fragment molecular orbital (FMO) method, in which each fragment contains the side chain of corresponding amino acid residue. We have carried out the FMO-MP2 (second-order Moeller–Plesset) calculation for the complex of HA antigen and Fab antibody of influenza virus H3N2 A/Aichi/2/68 and obtained the IFIE values between each amino acid residue in HA and the whole antibody as the sums over the residues contained in the latter. Combining this IFIE data with experimental data for hemadsorption activity of HA mutants, we succeeded in theoretically explaining the mutations in HA observed after the emergence of influenza virus H3N2 A/Aichi/2/68 in an earlier study, except for those of THR83. In the present study, we employ an alternative way of fragment division in the FMO calculation at the carbonyl C site of the peptide bond instead of the C_α site used in the previous work, which provides revised IFIE values consistent with all the historical mutation data in the antigenic region E of HA including the case of THR83 in the present prediction scheme for probable mutations in HA.

Keywords Influenza virus · Hemagglutinin · Antibody · Fragment molecular orbital · Inter-fragment interaction energy

Dedicated to Professor Akira Imamura on the occasion of his 77th birthday and published as part of the Imamura Festschrift Issue.

A. Yoshioka · S. Tanaka (✉)
Graduate School of System Informatics, Kobe University, 1-1 Rokkodai, Nada-ku, Kobe 657-8501, Japan
e-mail: tanaka2@kobe-u.ac.jp

K. Takematsu · S. Tanaka
Graduate School of Human Development and Environment, Kobe University, 3-11 Tsurukabuto, Nada-ku, Kobe 657-8501, Japan

I. Kurisaki · S. Tanaka
Graduate School of Science and Technology, Kobe University, 1-1 Rokkodai, Nada-ku, Kobe 657-8501, Japan

K. Fukuzawa
Mizuho Information and Research Institute Inc., 2-3 Kanda Nishiki-Cho, Chiyoda-ku, Tokyo 101-8443, Japan

Y. Mochizuki
Department of Chemistry and Research Center for Smart Molecules, Faculty of Science, Rikkyo University, 3-34-1 Nishi-ikebukuro, Toshima-ku, Tokyo 171-8501, Japan

T. Nakano
Division of Medicinal Safety Science, National Institute of Health Sciences, 1-18-1 Kamiyoga, Setagaya-ku, Tokyo 158-8501, Japan

E. Nobusawa
National Institute of Infectious Diseases, 1-23-1 Toyama, Shinjuku-ku, Tokyo 162-8640, Japan

K. Nakajima
Department of Virology, Medical School, Nagoya City University, 1 Kawasumi, Mizuho-cho, Mizuho-ku, Nagoya 467-8601, Japan

Abbreviations

HA	Hemagglutinin
FMO	Fragment molecular orbital
IFIE	Inter-fragment interaction energy
MP2	Moeller–Plesset second-order perturbation

1 Introduction

Hemagglutinin (HA), a major antigenic protein of the influenza virus, is a homo-trimeric glycoprotein situated on the viral surface [1]. HA plays an important role in the early stage of infection such as the binding to the receptors (sialic acids) on the host cells and the trigger for the fusion between virus and endosome membranes. The receptor-binding site (RBS) is located on the membrane-distal globular domain of HA. The neutralizing antibody targeting the antigenic regions located around the RBS then prohibits the virus from binding to the receptors. Antigenic variants are generally selected during circulation of the viruses among human population [2]. In these variants (mutants), amino acid differences are observed in the antigenic regions compared to the original viruses. The structural analyses of HA-antibody complexes have provided the information about the amino acid residues on HA directly interacting with the antibody in the complexes. Amino acid changes (mutations) at these positions allow the virus to escape from the neutralizing antibody.

In an earlier study [3], we performed a quantum-chemical, electron-correlated second-order Moeller–Plesset (MP2) perturbation calculation [4] for the HA antigen–antibody system of influenza virus H3N2 A/Aichi/2/68 [5] with the fragment molecular orbital (FMO) method [6, 7], in which a large antigen–antibody biomolecular system was divided into a collection of many fragments corresponding to amino acid residues. On the basis of the calculated inter-fragment interaction energies (IFIEs) [8–14] representing the molecular interactions between the amino acid residues in the antigen–antibody complex, we identified those residues in the antigenic region E [15, 16] of HA protein that were significantly recognized by the Fab fragment of antibody [17, 18] with strongly attractive interactions. Combining these IFIE results with the data of hemadsorption experiments [19, 20] by which the mutation-prohibited sites were specified enabled us to explain most of those mutation sites actually observed (five of six residues) as a benchmark test, which would thus provide a promising method for predicting the HA residues that have a high probability of forthcoming mutation.

In spite of its success, only one residue site in HA has remained to be explained in the earlier study [3], whose mutation cannot be accounted for appropriately in terms of the proposed prediction scheme. That is the THR83 in the antigenic region E of HA, which shows a repulsive interaction with the Fab antibody in the FMO calculation, but has mutated three times [19, 20] after the emergence of the H3N2 influenza virus in 1968. In our prediction method, the amino acid residue that shows an attractive interaction with the antibody was supposed to have a high probability for mutation in order to escape from antibody recognition. One of the possible reasons for the disagreement with the observation can be ascribed to the fragment division method employed in the FMO calculation. We relied on the fragment division at the C_α site in the polypeptide chain according to the usual FMO recipe [6, 7, 21] for reducing the computational error in total energy, while this method of fragmentation may be less natural than the division at the peptide bond in light of biochemical function (see also the Sect. 4 below). Therefore, we here attempt an alternative method of fragment division for the IFIE calculation in the FMO method to overcome this difficulty. Concerning the accuracy of the calculated energies, the fragment division at the atoms other than the C_α site may cause additional energy errors in IFIEs by the order of less than 1 kcal/mol [6, 7, 21]. (Note that the IFIE values calculated with different fragmentations differ mainly due to the difference in the fragment units employed in the FMO calculations.)

The present article is organized as follows. In Sect. 2, the models and methods employed in the present study are illustrated. The calculated results obtained by the two kinds of the fragmentations are shown and compared in Sect. 3. We thus find in Sect. 4 that the IFIEs calculated through the fragmentation at the peptide bond give a description for the antigen–antibody interactions, which is more consistent with the main stream amino acid changes observed in the antigenic region E of HA. Section 5 concludes with a summary.

2 Models and methods

We employ an HA-Fab antigen–antibody system of H3N2 A/Aichi/2/68 influenza virus (PDB ID: 1EO8) [5] in the present analysis. Before performing the FMO-IFIE calculations, we added the missing hydrogen atoms in the complex and optimized their positions with the aid of MMFF94x force field [22] on the MOE (Molecular Operating Environment, Chemical Computing Group Inc.) software. Then, the FMO-MP2/6-31G* [3, 4] and the corresponding classical force-field (Amber ff99 [23]) calculations have been carried out for the antigen–antibody complex with 921 residues and 14,086 atoms, in which the monomer structure of HA [5] is employed. In contrast to

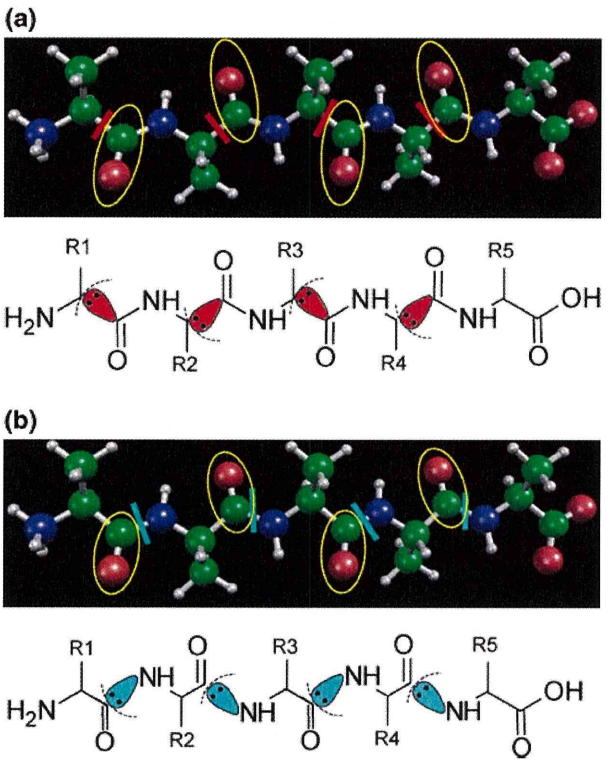

Fig. 1 Two methods of fragment division for the polypeptide chain. **a** The fragment division at the C_α site employed in the usual FMO calculations. **b** The fragment division at the carbonyl C site of the peptide bond employed in the present study. In the *lower panels*, the *dotted line* shows the fragmentation border, where chemical bond (orbital marked in *red* or *blue*) and electrons (represented by *dots*) are partitioned according the conventional FMO recipe [6, 7, 21]

the earlier study, where the fragmentation was performed at the C_α site of the C–C bond according to the usual FMO prescription [6, 7, 21], the fragmentation is performed at the carbonyl C site of the peptide (C–N) bond in the present analysis. The comparison between these two methods of the fragmentation is illustrated in Fig. 1.

We obtained the IFIEs [8–14] on the bases of these force-field and FMO (two-body FMO expansion [21] in this study) calculations and summed the values of IFIEs over the residues contained in the antibody. It is noted here that the IFIE is equivalent to the pair interaction energy (PIE) employed in other FMO studies [21]. These IFIE sums for each antigenic region A–E demonstrate that the amino acid residues in the vicinity of the antigenic region E are significantly recognized by the antibody through strongly attractive interactions, indicating that these residues are highly responsible for the binding affinity between the HA antigen and the Fab fragment of antibody. We therefore focus on 24 residues in the vicinity of the antigenic region E (residue numbers 62–85) in the present analysis.

It is noted, in passing, that we employ in this study an energetically optimized structure of complex on the basis of the PDB (Protein Data Bank) registered structure as a representative snapshot. Structural fluctuations of protein complex in environmental solvent are thus neglected in the present analysis, which may be justified by the consideration that the optimized structure should be observed dominantly by the energetical reason. It is also supposed that the screening effect due to solvent [24] would not change the relative order or the sign of IFIEs. In this regard, the MP2 electron-correlation method [3, 4, 8–14] is employed in the FMO calculation in order to appropriately describe the weak dispersion interactions in addition to other quantum-mechanical effects such as electronic polarization and charge transfer.

3 Calculated results

First, we show the result for the IFIEs between each residue in HA and the Fab fragment of antibody obtained by the classical force-field calculation, in which the fragmentation is performed at the carbonyl C site of the peptide bond. Figure 2a–c demonstrate the calculated results for charged, hydrophobic and polar residues in the antigenic region E, respectively, in comparison with the earlier FMO results to which the fragmentation at the C_α site was applied. As seen in the figures, the qualitative tendency of the interactions is well correlated in both calculations on the whole, while the classical force-field calculation seems to underestimate the contribution associated with the attractive dispersion interaction; the differences for the charged residues may be partially ascribed to the neglects of electronic polarization and charge transfer in the classical calculation. A significant, qualitative difference between the two calculations is then observed for those residues such as GLN80 and THR83, which may be attributed to the difference in the ways of fragment division as mentioned earlier. In particular, the latter residue is important in the present context of mutation prediction. If we would employ the IFIE value between THR83 and antibody obtained through the force-field calculation, we can assign this residue as a probable candidate for forthcoming mutation because the mutation at the THR83 site could diminish the currently attractive interaction with the antibody, which would be favorable for the escape from the antibody pressure. This is then consistent with the observation [19, 20] that the THR83 site has undergone mutations in the actual influenza viruses.

We have next carried out the FMO-MP2/6-31G* calculation for the identical antigen–antibody structure. In this calculation, we have modified the method of fragmentation from that employed in the earlier work, so that five residues including THR83 are separated at the carbonyl C site of the

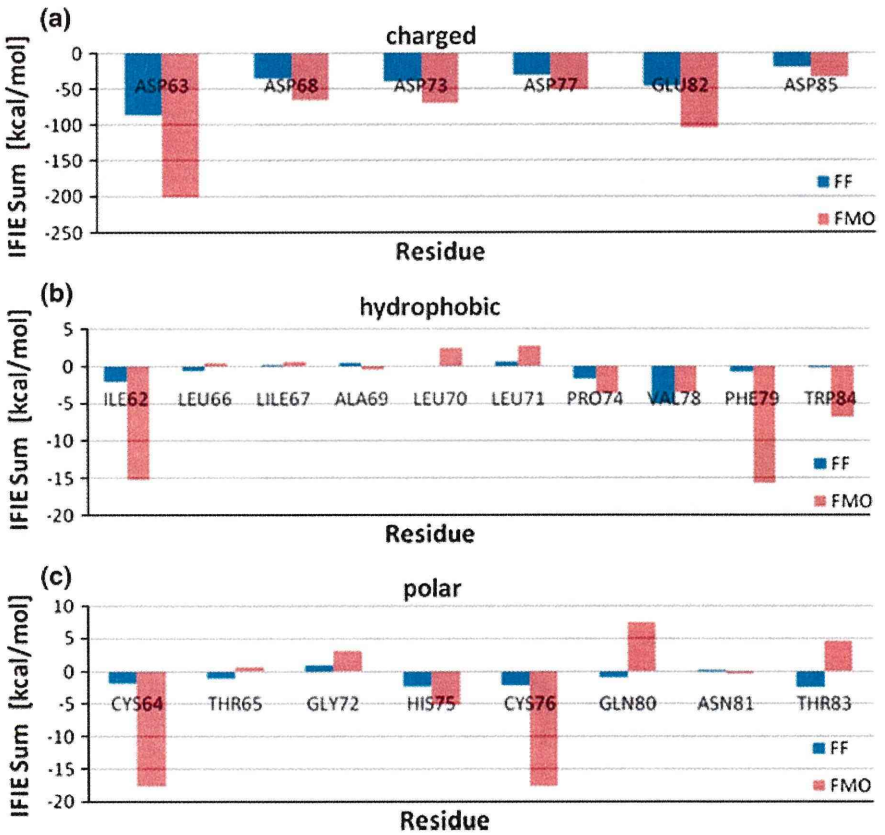

Fig. 2 IFIE values between the whole Fab antibody and each amino acid residue in HA. The *blue* and *red bars* represent the results obtained by the classical force-field (FF) calculation with the present fragmentation of Fig. 1b and by the FMO-MP2/6-31G* calculation with the usual (previous) FMO fragmentation of Fig. 1a, respectively. **a** Charged residues. **b** Hydrophobic residues. **c** Polar residues

peptide bond instead of the C_α site. Table 1 shows the IFIE values between each residue fragment and the antibody, which are compared between the previous and present ways of FMO fragmentation. Most interesting in this table is the IFIE values for THR83 and TRP84. The IFIE for THR83 changes from 4.52 kcal/mol in the previous scheme to −4.93 kcal/mol in the present scheme, which is in line with the result observed in the classical force-field calculation above; on the other hand, that for TRP84 changes from −6.85 to 1.25 kcal/mol. These results can be accounted for as consequences of the modification of the fragmentation, as will be addressed in the following section, and provide a consequence consistent with the observation [19, 20] for mutations of HA in the H3N2 influenza virus.

4 Discussion

As addressed in Sect. 2, the fragment assignment of the carbonyl group C=O in the main chain of polypeptide is different between the two types of fragmentations shown in Fig. 1; the fragmentation was performed at the C_α site in the usual FMO scheme, while it is performed at the carbon site of the carbonyl group C=O constituting the peptide bond in the scheme proposed in the present study. When we consider the IFIE between THR83 in HA and ARG98 in Fab antibody, this difference causes a significant consequence. Figure 3 illustrates the configuration of THR83 and ARG98 in the antigen–antibody complex. The carbonyl group next to the side chain of THR83 has an attractive interaction with ARG98. In the case of original FMO fragmentation, this carbonyl group belongs to the fragment containing the side chain of TRP84, then bringing about an attractive IFIE between the TRP84 fragment and the antibody (see −6.85 kcal/mol in Table 1). In the present fragmentation, on the other hand, this carbonyl group belongs to the fragment containing the side chain of THR83. Thus, the IFIE value between the THR83 fragment and the antibody becomes negative (−4.93 kcal/mol) in the present FMO calculation, as seen in Table 1, providing a calculated result consistent with the mutation data in terms of the present prediction scheme.

It is noted that the mutations at all six residue sites, which have been observed in the antigenic region E of HA of H3N2 A/Aichi/2/68, can thus be accounted for by the prediction method based on the present fragmentation scheme. This example would suggest that the fragmentation at the carbonyl site of the peptide bond may be a more natural way of fragment division in FMO calculation in

Table 1 IFIE values (in units of kcal/mol) between the Fab antibody and amino acid residues in the vicinity of THR83

Fragment	IFIE sum (kcal/mol)	Number of atoms
(a) Previous		
GLN80	7.47	17
ASN81	−0.45	14
GLU82	−102.51	15
THR83	4.52	14
TRP84	−6.85	24
ASP85	−34.93	12
LEU86	2.21	19
(b) Present		
GLN80	7.43	17
ASN81	0.63	16
GLU82	−101.98	15
THR83	−4.93	14
TRP84	1.25	24
ASP85	−37.41	10
LEU86	2.23	19

(a) The results obtained by FMO-MP2/6-31G* calculation employing the usual fragment division at the C_α site of the C–C bond shown in Fig. 1a. (b) The results obtained by FMO-MP2/6-31G* calculation employing the present fragment division at the carbonyl C site of the peptide (C–N) bond shown in Fig. 1b. The numbers of atoms contained in each fragment corresponding to amino acid residue (side chain) are also shown

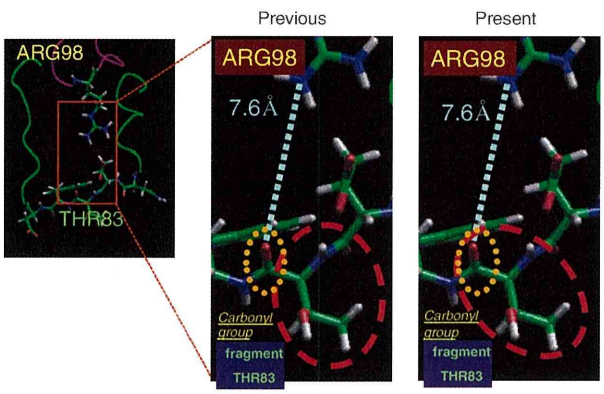

Fig. 3 Configuration of THR83 in HA antigen and ARG98 in Fab antibody. The side chain of THR83 and the carbonyl group interacting with ARG98 are *circled* by the *dashed red line* and the *dotted yellow line*, respectively. These two parts are contained in an identical fragment (THR83) only in the present fragmentation scheme

order to discuss biochemical consequences of mutations, while the original method of fragment division was employed to reduce the computational errors due to the fragmentation as much as possible in the FMO calculations [6, 7, 21]. In this connection, we suppose that the change of the side chain of amino acid residue would modify the local structure of neighboring region of the main chain as well, thus leading to the change in the interaction associated with the main chain. Thus, the effects of the mutations are indirect when the interactions associated with the main chain are important.

For more realistic analysis, we may employ the trimer structure [1] of HA antigen complexed with the Fab dimer antibody. The FMO calculations for this HA trimer system has already been performed [25] at the MP2 and MP3 levels. The prediction of mutations using this FMO-IFIE result and its comparison with that by HA monomer would be interesting, which will be reported elsewhere [26]. It is also remarked that the effect of fluctuating protein structures in aqueous solution on the antigen–antibody interaction [27], which is beyond the scope of the present study, is an issue to be investigated in the future.

5 Conclusion

Our prediction scheme for probable mutations in HA protein of influenza virus depends on the evaluation of interactions between amino acid residues in HA and associated antibody. If the interaction is attractive, the corresponding residue would have a higher probability of forthcoming mutation in order to mitigate the molecular recognition by the antibody. These interaction energies could be evaluated in terms of the IFIEs obtained through the FMO calculation for the antigen–antibody complex. Then, the method of the fragment division employed in the FMO calculation would be important in order to appropriately assign the local interactions associated with pertinent groups in amino acid residues to each fragment. It is noted that these fragmentations are somewhat empirical and lead to the arbitrariness in the IFIE values. In our previous analysis [3] on an HA antigen–antibody system, we relied on the conventional fragmentation scheme in the FMO calculation and found that the prediction scheme worked well for explaining five of the six past mutations in the HA of H3N2 A/Aichi/2/68 influenza virus, but leaving the mutations of THR83 unexplained. In the present study, on the other hand, we have performed a novel fragmentation at the carbonyl C site of the peptide bond, which is more consistent with the biochemical importance of the peptide bond moiety in protein structures. While this fragmentation may bring about increased errors of calculated energies in the FMO approximation, we have improved the agreement between the theoretical prediction and the past mutations observed in the antigenic region E of HA of H3N2 A/Aichi/2/68 influenza virus. This finding may thus suggest various options [28] for us to choose the method of fragmentation employed in the FMO calculation according to the purpose of analysis.

Acknowledgments This work was partially supported by the CREST project of Japan Science and Technology Agency (JST) and by the Health and Labour Sciences Research Grants on Emerging and Re-emerging Infectious Diseases (No. H22-Shinko-Ippan-006) from the Ministry of Health, Labour and Welfare of Japan.

References

1. Barbey-Martin C, Gigant B, Bizebard T, Calder LJ, Wharton SA, Skehel JJ, Knossow M (2002) Virol 294:70
2. Russell CA et al (2008) Science 320:340
3. Takematsu K, Fukuzawa K, Omagari K, Nakajima S, Nakajima K, Mochizuki Y, Nakano T, Watanabe H, Tanaka S (2009) J Phys Chem B 113:4991
4. Mochizuki Y, Yamashita K, Murase T, Nakano T, Fukuzawa K, Takematsu K, Watanabe H, Tanaka S (2008) Chem Phys Lett 457:396
5. Fleury D, Daniels RS, Skehel JJ, Knossow M, Bizebard T (2000) Struct Funct Gen 40:572
6. Kitaura K, Ikeo E, Asada T, Nakano T, Uebayasi M (1999) Chem Phys Lett 313:701
7. Nakano T, Kaminuma T, Sato T, Akiyama Y, Uebayasi M, Kitaura K (2000) Chem Phys Lett 318:614
8. Fukuzawa K, Komeiji Y, Mochizuki Y, Kato A, Nakano T, Tanaka S (2006) J Comput Chem 27:948
9. Fukuzawa K, Mochizuki Y, Tanaka S, Kitaura K, Nakano T (2006) J Phys Chem B 110:16102
10. Kurisaki I, Fukuzawa K, Komeiji Y, Mochizuki Y, Nakano T, Imada J, Chmielewski A, Rothstein SM, Watanabe H, Tanaka S (2007) Biophys Chem 130:1
11. Ito M, Fukuzawa K, Mochizuki Y, Nakano T, Tanaka S (2007) J Phys Chem B 111:3525
12. Ito M, Fukuzawa K, Mochizuki Y, Nakano T, Tanaka S (2008) J Phys Chem A 112:1986
13. Ito M, Fukuzawa K, Ishikawa T, Mochizuki Y, Nakano T, Tanaka S (2008) J Phys Chem B 112:12081
14. Iwata T, Fukuzawa K, Nakajima K, Aida-Hyugaji S, Mochizuki Y, Watanabe H, Tanaka S (2008) Comput Biol Chem 32:198
15. Wiley DC, Wilson IA, Skehel JJ (1981) Nature 289:373
16. Skehel JJ, Stevens DJ, Daniels RS, Douglas AR, Knossow M, Wilson IA, Wiley DC (1984) Proc Natl Acad Sci USA 81:1779
17. Bizebard T, Mauguen Y, Petek F, Rigolet P, Skehel JJ, Knossow M (1990) J Mol Biol 216:513
18. Gigant B, Fleury D, Bizebard T, Skehel JJ, Knossow M (1995) Proteins 23:115
19. Nakajima K, Nobusawa E, Tonegawa K, Nakajima S (2003) J Virol 77:10088
20. Nakajima K, Nobusawa E, Nagy A, Nakajima S (2005) J Virol 79:6472
21. Fedorov DG, Kitaura K (2009) The fragment molecular orbital method. CRC Press, Boca Raton
22. Halgren TA (1996) J Comput Chem 17:490
23. Case DA, Cheatham TE, Darden T, Gohlke H, Luo R, Merz KM, Onufriev A, Simmerling C, Wang B, Woods RJ (2005) J Comput Chem 26:1668
24. Watanabe H, Okiyama Y, Nakano T, Tanaka S (2010) Chem Phys Lett 500:116
25. Mochizuki Y, Yamashita K, Fukuzawa K, Takematsu K, Watanabe H, Taguchi N, Okiyama Y, Tsuboi M, Nakano T, Tanaka S (2010) Chem Phys Lett 493:346
26. Yoshioka A, Fukuzawa K, Mochizuki Y, Yamashita K, Nakano T, Okiyama Y, Nobusawa E, Nakajima K, Tanaka S (2011) J Mol Graph Model 30:110
27. Zhou R, Das P, Royyuru AK (2008) J Phys Chem B 112:15813
28. Tamura K, Inadomi Y, Nagashima U (2007) Bull Chem Soc Jpn 80:721

Journal of Molecular Graphics and Modelling 30 (2011) 110–119

Contents lists available at ScienceDirect

Journal of Molecular Graphics and Modelling

journal homepage: www.elsevier.com/locate/JMGM

Prediction of probable mutations in influenza virus hemagglutinin protein based on large-scale ab initio fragment molecular orbital calculations

Akio Yoshioka[a], Kaori Fukuzawa[b], Yuji Mochizuki[c], Katsumi Yamashita[d], Tatsuya Nakano[e], Yoshio Okiyama[f], Eri Nobusawa[g], Katsuhisa Nakajima[h], Shigenori Tanaka[a,*]

[a] Graduate School of System Infrormatics, Kobe University, 1-1, Rokkodai, Nada-ku, Kobe 657-8501, Japan
[b] Mizuho Information and Research Institute, Inc., 2-3, Kanda Nishi-cho, Chiyoda-ku, Tokyo 101-8443, Japan
[c] Department of Chemistry and Research Center for Smart Molecules, Faculty of Science, Rikkyo University, 3-34-1, Nishi-Ikebukuro, Toshima-ku, Tokyo 171-8501, Japan
[d] 1st Manufacturing Industries Solutions Division, NEC Soft Ltd., 1-18-6, Shinkiba, Koto-ku, Tokyo 136-8608, Japan
[e] Division of Safety Information on Drug, Food and Chemicals, National Institute of Health Sciences, 1-18-1, Kamiyoga, Setagaya-ku, Tokyo 158-8501, Japan
[f] Institute of Industrial Science, The University of Tokyo, 4-6-1, Komaba, Meguro-ku, Tokyo 153-8505, Japan
[g] National Institute of Infectious Diseases, Toyama 1-23-1, Shinjuku-ku, Tokyo 162-8640, Japan
[h] Department of Virology, Medical School, Nagoya City University, 1, Kawasumi, Mizuho-cho, Mizuho-ku, Nagoya 467-8601, Japan

ARTICLE INFO

Article history:
Received 22 April 2011
Received in revised form 24 June 2011
Accepted 27 June 2011
Available online 6 July 2011

Keywords:
Influenza
Hemagglutinin (HA)
Antibody
Mutation
Fragment molecular orbital (FMO) method

ABSTRACT

Ab initio electronic-state calculations for influenza virus hemagglutinin (HA) trimer complexed with Fab antibody were performed on the basis of the fragment molecular orbital (FMO) method at the second and third-order Møller–Plesset (MP2 and MP3) perturbation levels. For the protein complex containing 2351 residues and 36,160 atoms, the inter-fragment interaction energies (IFIEs) were evaluated to illustrate the effective interactions between all the pairs of amino acid residues. By analyzing the calculated data on the IFIEs, we first discussed the interactions and their fluctuations between multiple domains contained in the trimer complex. Next, by combining the IFIE data between the Fab antibody and each residue in the HA antigen with experimental data on the hemadsorption activity of HA mutants, we proposed a protocol to predict probable mutations in HA. The proposed protocol based on the FMO-MP2.5 calculation can explain the historical facts concerning the actual mutations after the emergence of A/Hong Kong/1/68 influenza virus with subtype H3N2, and thus provides a useful methodology to enumerate those residue sites likely to mutate in the future.

1. Introduction

Hemagglutinin (HA), a major antigenic protein of the influenza virus, is a homo-trimeric glycoprotein. HA plays an important role in the early stage of infection; binding to the receptors (sialic acids) on the host cells and trigger for the fusion between virus and endosome membranes. The receptor binding site (RBS) locates on the membrane-distal globular domain of HA. The neutralizing antibody targeting antigenic regions located around RBS prohibits the virus from binding to the receptors [1,2]. Antigenic variants are generally selected during circulation of the viruses among human population. In these variants, amino acid differences are observed in the antigenic region compared to the original viruses [3]. The structural analyses of HA–antibody complexes have provided the information about the amino acid residues on HA directly interacting with the antibody in the complexes. Amino acid substitutions at these sites allow the virus to escape from the neutralizing antibody [4–6].

In this paper, we first specify the sites of the antigenic region under the antibody pressure based on the X-ray structure of complex of the HA A/Hong Kong/1/68 (H3N2) with the antibody HC63 [7]. This structure is a complex of HA trimer and fragment of antigen binding (Fab) dimer. The pandemic of human influenza in 1968 was caused by the viruses that were human/avian virus reassortants [8]. Moreover, this virus often has undergone antigenic drifts after this outbreak [9]. We may further be faced with influenza pandemics by the causes of antigenic shift with the highly lethal viruses and antigenic drift in the future.

To predict the probable mutation sites of the antigenic region in HA, in an earlier work [10], we developed a practical scheme by combining the inter-fragment interaction energy (IFIE) analysis of fragment molecular orbital (FMO) method with experimental information about the hemadsorption activity of mutants [11,12], in which an HA monomer structure [6] was used. However, it was indicated [7] that the Fab monomer can effectively recognize not only directly linked (e.g., Fab(I) versus HA(I) or Fab(II) versus HA(II))

* Corresponding author. Tel.: +81 78 803 6620; fax: +81 78 803 6621.
E-mail address: tanaka2@kobe-u.ac.jp (S. Tanaka).

1093-3263/$ – see front matter © 2011 Elsevier Inc. All rights reserved.
doi:10.1016/j.jmgm.2011.06.011